ORIGINAL PAPER

Helical surfaces with a constant ratio of principal curvatures

Yang Liu[1] · Olimjoni Pirahmad[1] · Hui Wang[1] · Dominik L. Michels[1] ·
Helmut Pottmann[1] (ID)

© The Managing Editors 2022

Abstract

We determine all helical surfaces in three-dimensional Euclidean space which possess a constant ratio $a := \kappa_1/\kappa_2$ of principal curvatures (CRPC surfaces), thus providing the first explicit CRPC surfaces beyond the known rotational ones. Our approach is based on the involution of conjugate surface tangents and on well chosen generating profiles such that the characterizing differential equation is sufficiently simple to be solved explicitly. We analyze the resulting surfaces, their behavior at singularities that occur for $a > 0$, and provide an overview of the possible shapes.

Keywords Helical surface · Surface with a constant ratio of principal curvatures · Weingarten surface

Mathematics Subject Classification 53A05 · 53A10 · 53C42

1 Introduction

Surfaces which possess a relation $F(\kappa_1, \kappa_2) = 0$ between their principal curvatures κ_1, κ_2 are named after Weingarten (1861) who studied them in connection with a characterization of those surfaces that are isometric to rotational surfaces. The latter are exactly the focal surfaces of Weingarten surfaces. There has been a huge interest in important special cases, such as surfaces with constant Gaussian or mean curvature, but apart from those, there are only very few explicitly known Weingarten surfaces.

In this paper, we contribute to surfaces in Euclidean $\mathbb{R}^3$ which possess a constant ratio of principal curvatures $\kappa_1/\kappa_2 =: a$. We exclude surfaces with one vanishing principal curvature (developable surfaces) and call the others *CRPC surfaces*. CRPC surfaces are a natural generalization of minimal surfaces ($a = -1$). However, in big contrast to minimal surfaces, very little is known about them. Explicit parameteri-

---

✉ Helmut Pottmann
  helmut.pottmann@kaust.edu.sa

1 KAUST Visual Computing Center, King Abdullah University of Science and Technology, Thuwal
   23955-6900, Saudi Arabia

 ⌀ Springer

zations are only available for rotational CRPC surfaces (Hopf [1951](#); Kühnel [2013](#); Mladenov and Oprea [2003](#), [2007](#); Lopez and Pampano [2020](#); Wang and Pottmann [2022](#)). Lopez and Pampano ([2020](#)) recently presented a classification of all rotational surfaces with a linear relation $\kappa_1 = a\kappa_2 + b$ between principal curvatures, including a study of the special case $b = 0$ of CRPC surfaces. Their work also contains a variational characterization of the profiles of these surfaces. Rotational CRPC surfaces with $K < 0$ have also been characterized via isogonal asymptotic parameterizations $f(u, v)$ where $|f_u| = |f_v|$ (Riveros and Corro [2012](#), [2013](#); Stäckel [1896](#)). Moreover, it has been shown that Weingarten surfaces to a linear relation of the form $a\kappa_1 + b\kappa_2 + c = 0$ are rotational if they are foliated by a family of circles (López [2008](#)).

Jimenez et al. ([2020](#)) derived CRPC surfaces via a Christoffel-type transformation of certain spherical nets, with a focus on discrete models. Effective methods for the computation of discrete CRPC surfaces (Wang and Pottmann [2022](#)) provided some insight on the shape variety of CRPC surfaces. As these are based on numerical optimization, one cannot derive precise mathematical conclusions, but conjectures as basis for further studies.

To add new explicit representations of CRPC surfaces beyond the rotational ones, one will look into other special surface classes. Unfortunately, some classes are excluded quickly: A *ruled CRPC surface* has the rulings as one family of asymptotic curves and the other family of asymptotic curves needed to intersect the rulings under a constant angle. The set of second asymptotic directions $A(t)$ along a ruling R is a regulus on a ruled quadric. This contradicts a constant angle between R and $A(t)$ except for a right angle, leading to the helicoid as ruled minimal surface. One can also apply a result by Kühnel ([2013](#)), which states that ruled Weingarten surfaces are helical or rotational, and check that there are no CRPC surfaces among them except helicoids. Likewise, channel surfaces (envelopes of one-parameter families of spheres) can only be Weingarten surfaces if they are rotational surfaces or helical pipe surfaces, so that the only CRPC channel surfaces are just the rotational ones.

In this paper, we explicitly determine all *helical CRPC surfaces*. Clearly, this amounts to solving a 2nd order ordinary differential equation and may seem like a simple exercise. However, this ODE turns out to be very complicated even for natural choices of profile curves, such as intersections with planes through the helical axis or orthogonal to it.

We show how to choose proper generating curves of the helical surfaces so that the ODE is sufficiently simple and can be solved explicitly. We do not compute principal curvatures for setting up the ODE, but work only with the involution of conjugate surface tangents. Profiles are chosen so that they directly contribute to the determination of this involution. Our approach works with a parameter that is agnostic to the change from curvature ratio a to $1/a$, resolving the difficulty in distinguishing between the two principal curvature directions on a helical surface.

The explicit representation of all helical CRPC surfaces (Theorem [3](#)) is then studied from different viewpoints. In particular, we investigate the singularities that appear for positive curvature, and we classify the potential shapes. Remarkably, there is a way to distinguish between CRPC surfaces with ratio a and $1/a$ for $a > 0$, and we show that this ratio switches at the singularities.

By the way, the existence of singularities could only be expected, but not be shown at the discrete models in Wang and Pottmann (2022). Finally, we mention that our interest in CRPC surfaces originated from various applications in freeform architecture (Pellis et al. 2021b; Schling et al. 2018; Tellier et al. 2020).

2 Deriving the characterizing differential equation

2.1 CRPC surfaces via the involution of conjugate tangents

Surfaces with a constant ratio $a = \kappa_1/\kappa_2$ of principal curvatures κ_1, κ_2 with $\kappa_i \neq 0$, can be characterized by the involution of conjugate surface tangents at each of its points. In the principal frame at a surface point, the involution between conjugate tangent vectors (x_1, x_2) and $(\bar{x}_1, \bar{x}_2)$, is given by $\kappa_1 x_1 \bar{x}_1 + \kappa_2 x_2 \bar{x}_2 = 0$. In our case, it reads

$$ax_1\bar{x}_1 + x_2\bar{x}_2 = 0. \tag{1}$$

Principal tangents $(1, 0)$, $(0, 1)$ are conjugate to each other. Asymptotic tangents $(1, \pm\sqrt{-a})$ are self-conjugate, but real only for Gaussian curvature $K = \kappa_1\kappa_2 < 0$. For $K > 0$, tangents $(1, \pm\sqrt{a})$ are conjugate to each other and symmetric with respect to the principal directions. For positive and negative curvature, we define $(1, \pm\sqrt{|a|})$ as *characteristic tangents*. Then, *a CRPC surface is characterized by a constant angle 2α between the characteristic tangents at all surface points*, where $\tan\alpha = \sqrt{|a|}$.

We now apply a method of constructive projective geometry, by intersecting the pencil of surface tangents at a surface point p with a circle c_s (Steiner circle; center m_s, radius r_s) that passes through p and lies in the tangent plane $\tau(p)$ at p (see Fig. 1, left). Each tangent T intersects c_s in two points: p and another point t'. The map $\pi : T \mapsto \bar{T}$ is transformed to an involution $\pi_s : t' \mapsto \bar{t}'$ on c_s, and lines $t'\bar{t}'$ pass through a fixed point (involution center) I_s.

Lemma 1 *A surface with constant principal curvature ratio $a = \kappa_1/\kappa_2$ is characterized as follows: At each surface point p, we project the involution of conjugate surface tangents onto a Steiner circle c_s. Then, the radius r_s of c_s and the distance d_s of the involution center I_s to the center m_s of c_s possess a constant ratio,*

$$k = \frac{d_s}{r_s} = \left|\frac{1-a}{1+a}\right| = \sqrt{1 - \frac{K}{H^2}}. \tag{2}$$

Proof For $K < 0$, I_s is outside c_s (Fig. 1, left, and I_s^- in Fig. 1, right) and the fixed points of π_s are the contact points of tangents from I_s to c_s. These points lie in the asymptotic tangents. For $K > 0$, the line through I_s which is orthogonal to $I_s m_s$ intersects c_s in points of the characteristic tangents (case I_s^+ in Fig. 1, right).

By elementary geometry, we have $|\cos 2\alpha| = d_s/r_s$ for $K > 0$ and $|\cos 2\alpha| = r_s/d_s$ for $K < 0$. Noting $\cos 2\alpha = (1 - \tan^2\alpha)/(1 + \tan^2\alpha)$ and that $\tan^2\alpha$ equals a for $K > 0$ and $-a$ for $K < 0$, we obtain (2). □

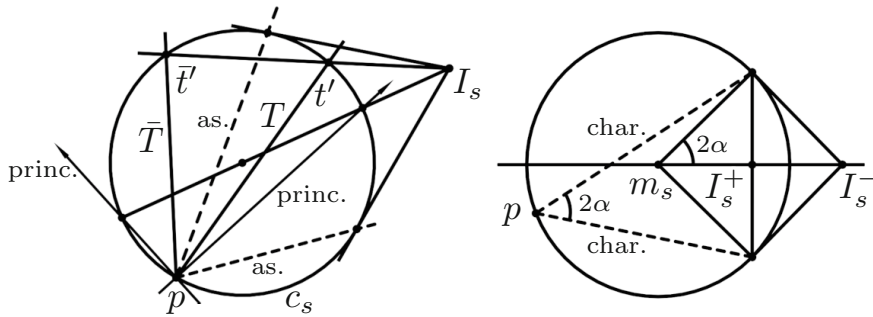**Fig. 1** Left: Involution of conjugate tangents at a point p, projected onto a circle c_s through p: corresponding points on c_s are collinear with the involution center I_s. Right: Relation between characteristic angle 2α and involution center I_s^+ (for $K > 0$) and I_s^- (for $K < 0$)

Remark 1 For most surfaces, also helical surfaces, there is no clear way to select one principal direction as the first one. Hence, it is an advantage that k is agnostic to that, which is also reflected in its expression via K and mean curvature H. Let us note the special cases which we are not interested in:

(a) Since neither plane nor sphere are helical, it is impossible to have $k = 0, a = 1$;
(b) Developable surfaces, i.e. $k = 1, a \in \{0, \infty\}$;
(c) Minimal surfaces, i.e. $k = \infty, a = -1$.

2.2 Application to helical surfaces

In Euclidean $\mathbb{R}^3$, we use Cartesian coordinates (x, y, z) and consider a helical motion about the z-axis with pitch p. It is composed of a continuous rotation with angular velocity 1 about the z-axis and a continuous translation with velocity p parallel to it. A point with initial position (x_0, y_0, z_0) generates a helical path, parameterized with the rotation angle v as

$$X(v) = (x_0 \cos v - y_0 \sin v, x_0 \sin v + y_0 \cos v, z_0 + pv), \ v \in \mathbb{R}.$$

A curve $X_0(t) = (x_0(t), y_0(t), z_0(t))$ generates a helical surface $X(v, t)$, which moves in itself under the helical motion. Thus, the same surface may be generated by any of its curves that is transversal to the helical paths. We use this freedom in choosing $X_0(t)$ to simplify the search for helical CRPC surfaces.

In the tangent planes of X we have to find two pairs of conjugate directions to set up the involution. For that, we recall the following geometric interpretation of conjugate directions. Given a curve c in a surface, we consider the envelope of tangent planes along c. This is a certain developable surface D. At each point of the curve c, the curve tangent T and the ruling $\bar{T}$ of D are conjugate tangents.

The tangent vector $T_p(X)$ of the helical path through a point X is $T_p(X) = (-y, x, p)$. It is well known that its conjugate direction $\bar{T}_p$ is the direction of steepest descent against the xy-plane Π, since the envelope of tangent planes along a helical

path is a developable helical surface whose rulings are lines of steepest descent in their tangent planes.

We now take as profile curve $X_0(t)$ one where the envelope D of tangent planes along it is simple. We choose D as a general cylinder with x-parallel rulings and write its tangent planes in the form $y = tz - f(t)$. This is no restriction, since the helical path tangents are never parallel to Π and thus no tangent plane of X and D can be parallel to Π (i.e. $t \neq \infty$).

The rulings of D arise by intersection of tangent planes with their derivative planes $z = f'(t)$, leading to the parameterization $D(t, w) = (w, tf' - f, f')$ of D. The curve $X_0(t) \subset D$ along which D is tangent to the helical surface X is the set of those points on D whose path tangents $(f - tf', w, p)$ are tangential to D, i.e. orthogonal to the normal $(0, 1, -t)$ of D. This yields $w = pt$,

$$X_0(t) = (pt, tf'(t) - f(t), f'(t)). \tag{3}$$

We call this curve the *contour* for projection parallel to the x-axis (or just contour for short) and use it as generating profile of a helical CRPC surface .

Lemma 2 *For a helical CRPC surface, the function f in the parameterization (3) of the contour satisfies the differential equation*

$$4p^2(1 + t^2) + ((1 + t^2)f'' + (tf' - f))^2 = k^2((1 + t^2)f'' - (tf' - f))^2. \tag{4}$$

Proof The contour tangents, $X_0' = (p, tf'', f'')$, are conjugate to $(1, 0, 0)$. The helical path tangent vectors at the contour are $(f - tf', pt, p)$, and they are conjugate to the directions of steepest descent in the tangent planes of D. We rotate each tangent plane of D (and X) at $X_0(t)$ about the x-parallel ruling of D so that it becomes parallel to the xz-plane. The new coordinates $(\tilde{x}, 0, \tilde{z})$ of tangent vectors are related to the original ones (x, y, z) by $(\tilde{x}, \tilde{z}) = \left(x, z\sqrt{1 + t^2}\right)$.

In the rotated position, we set up the involution of conjugate tangents and use a Steiner circle c_s with radius $r_s = \sqrt{1 + t^2}/2$ and center $m_s = (0, r_s)$ (see Fig. 2). The line of steepest descent ($\tilde{z}$-axis) corresponds to the path tangent $\tilde{T}_p$,

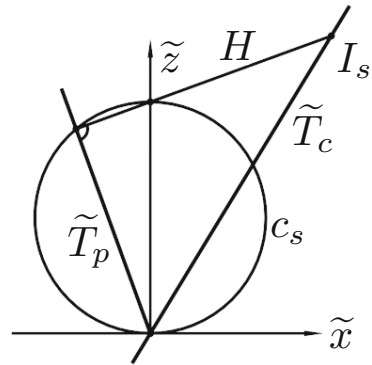$$(0, 1) \mapsto \left(f - tf', p\sqrt{1 + t^2}\right),$$

leading to line H through I_s, which passes through $(0, 2r_s)$ and is orthogonal to $\tilde{T}_p$,

$$H : (f - tf')\tilde{x} + p\sqrt{1 + t^2}\tilde{z} = p(1 + t^2).$$

The horizontal direction ($\tilde{x}$-axis) corresponds to the contour tangent $\tilde{T}_c$,

$$(1, 0) \mapsto \left(p, f''\sqrt{1 + t^2}\right).$$

Fig. 2 Constructing the involution center in a tangent plane of a helical CRPC surface

Since the $\tilde{x}$-axis touches c_s, $\tilde{T}_c$ contains the involution center I_s. Hence $I_s = H \cap \tilde{T}_c$,

$$I_s = \frac{1+t^2}{(1+t^2)f'' - (tf' - f)} \left(p, f''\sqrt{1+t^2} \right).$$

By Lemma 1, we have to express a constant ratio $k \geq 0$ between d_s and r_s, $\|I_s - m_s\|^2 = k^2 r_s^2$, which yields the characterizing differential Equ. (4). □

Remark 2 Since CRPC surfaces invariant under similarities, we can choose any pitch $p \neq 0$ and set $4p^2 = 1$. Thus in the rest of the paper, we only consider

$$1 + t^2 + ((1+t^2)f'' + (tf' - f))^2 = k^2((1+t^2)f'' - (tf' - f))^2. \tag{5}$$

Remark 3 *Helical minimal surfaces* are obtained with $k = \infty$ and therefore characterized by

$$(1+t^2)f'' - tf' + f = 0. \tag{6}$$

However, the derivation of this equation can be shortened a lot: The involution of conjugate tangents is the reflection at the (orthogonal) asymptotic directions. Since x-parallel and steepest tangent are orthogonal, the conjugate tangents, namely path tangent and contour tangent, must also be orthogonal. This yields (6), in which the pitch p does no longer appear. Hence the tangent cylinders orthogonal to the axis are the same as for rotational surfaces ($p = 0$), and one arrives at Wunderlich's generation of helical minimal surfaces as envelopes of a cylinder with a catenary as orthogonal cross section (Wunderlich 1952). Wunderlich derived these surfaces via Lie's generation of minimal surfaces as translation surfaces of conjugate complex isotropic curves. At its geometric core lies the fact that the isotropic tangents are conjugate to each other precisely for minimal surfaces.

3 Solution of the differential equation

Solving (5), we obtain the following parameterization of all helical CRCP surfaces.

Theorem 3 *Any helical surface X with a constant principal curvature ratio a is generated as follows. Let $k = \left| \frac{a-1}{a+1} \right|$ and functions $g(s), t(s)$ be defined by*

$$g(s) = \frac{(k-1)s^2 - (k+1)}{4ks} \sqrt{\frac{2Cs^{k+1}}{s^2+1}}, \quad t(s) = \sqrt{\frac{2Cs^{k+1}}{s^2+1} - 1}, \qquad (7)$$

where $s > 0, C > 0, 2Cs^{k+1} > s^2 + 1$. Let $H(v, \cdot)$ be the helical motion with pitch $1/2$,

$$H(v, (x_0, y_0, z_0)) = \left(x_0 \cos v - y_0 \sin v, \ x_0 \sin v + y_0 \cos v, \ z_0 + \frac{v}{2} \right).$$

Then X can be parameterized as

$$X(v, s) = 2pH(v, X_i(s)), \ s \in I_C, \ v \in \mathbb{R}, \ i = 0, 1,$$

where $X_i(s)$ is one of the following two curves,

$$X_0(s) = \left(\frac{t(s)}{2}, g(s), \int \frac{g'(s)}{t(s)} ds \right), X_1(s) = \left(-\frac{t(s)}{2}, g(s), -\int \frac{g'(s)}{t(s)} ds \right), \quad (8)$$

$I_C := \left\{ s : s > 0, \ \frac{2Cs^{k+1}}{s^2+1} > 1 \right\}$[1] and p is the pitch of X.

Proof By setting $g = tf' - f$ we can reduce ODE (5) to

$$1 + t^2 + \left(\left(t + \frac{1}{t} \right) g' + g \right)^2 = k^2 \left(\left(t + \frac{1}{t} \right) g' - g \right)^2. \qquad (9)$$

Further, letting $g = u\sqrt{1 + t^2}$ and noticing that $(t + \frac{1}{t})g' - g = \frac{u'}{t}(1 + t^2)^{\frac{3}{2}}$, we get

$$1 + \left(2u + \left(t + \frac{1}{t} \right) u' \right)^2 = k^2 \left(\left(t + \frac{1}{t} \right) u' \right)^2.$$

This leads us to a substitution for some function $s = s(t)$ such that

$$2u + \left(t + \frac{1}{t} \right) u' = \sinh(s), \quad k \left(t + \frac{1}{t} \right) u' = \cosh(s).$$

---

[1] We always assume that the constant C is large enough s.t. I_C is nonempty.

It immediately shows that

$$2u = \sinh(s) - \frac{\cosh(s)}{k} . \tag{10}$$

Taking the derivative and combining with the last formula in the substitution we obtain

$$s'(k - \tanh(s)) = \frac{2t}{1 + t^2} .$$

This equation is separable in variables and thus can be solved easily:

$$ks - \ln(\cosh(s)) + C' = \ln(1 + t^2) ,$$

or

$$t^2(s) = \frac{C e^{ks}}{\cosh(s)} - 1 ,$$

where C' is a constant and $C = e^{C'} > 0$. Together with Equ. (10) we obtain two parametric solutions for ODE (9), namely

$$g(s) = \frac{1}{2} \left(\sinh(s) - \frac{\cosh(s)}{k} \right) \sqrt{\frac{C e^{ks}}{\cosh(s)}}, \quad t(s) = \sqrt{\frac{C e^{ks}}{\cosh(s)} - 1}$$

and $(g(s), -t(s))$. Finally, since $g'(t) = t f''(t)$ and by total differentiation we have

$$\frac{g'(s)}{t'(s)} = g'(t) = t f''(t) = t(s) \frac{(f'(t))'_s}{t'(s)} .$$

Thus,

$$f'(t(s)) = \int \frac{g'(s)}{t(s)} ds .$$

Replacing e^s by s, we obtain the algebraic parameterizations in the theorem. $\qquad \square$

Two examples of helical CRPC surfaces based on this explicit representation and using the profile curve X_0 are shown in Fig. 3. It may seem that the two profile curves $X_0(s)$, $X_1(s)$ generate two different CRPC surfaces. However, we will now show that this is not really the case (Fig. 4).

Proposition 4 *The two curves $X_0(s)$, $X_1(s)$ in Equ. (8) generate two helical surfaces which can be joined to a single C^∞ CRPC surface.*
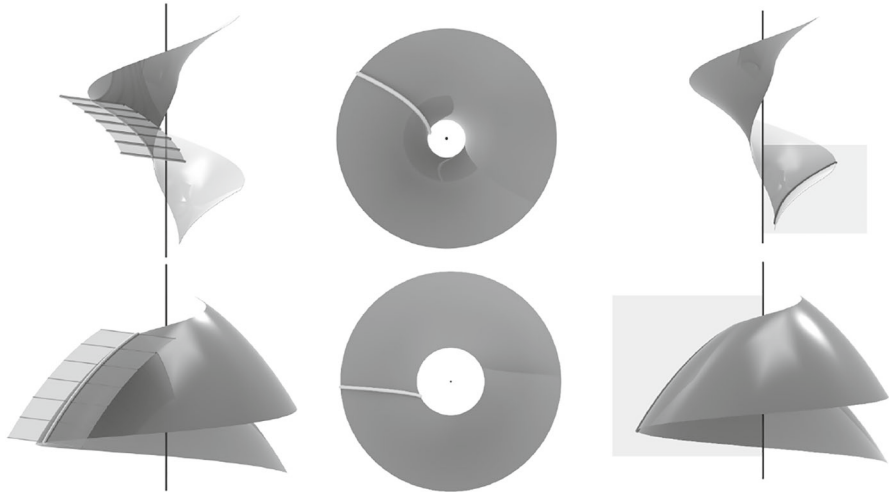
Fig. 3 Two helical CRPC surfaces generated by the profile curve X_0. The surface in the first row has a curvature ratio $a < 0$, the one in the 2nd row belongs to $a > 0$. 1st column: Cylinder surface tangent to the helical CRPC surface along X_0. 2nd column: Top view of X_0. 3rd column: Intersection with the xz-plane
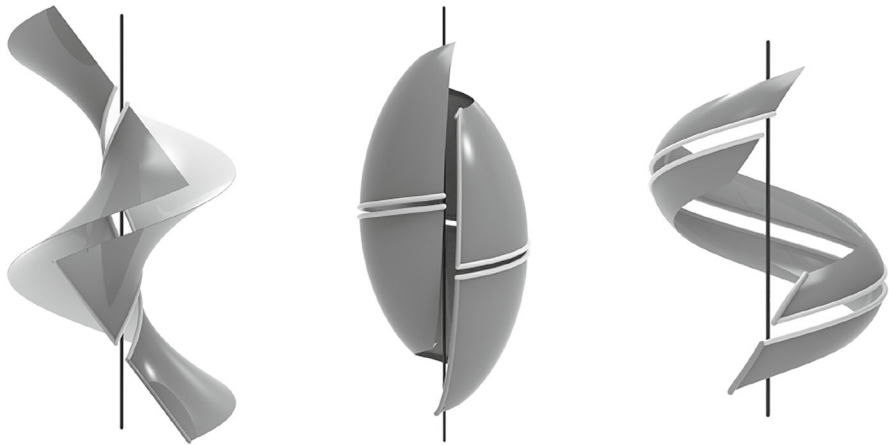

Fig. 4 The two curves X_0, X_1 given in Equ. (8) generate the upper half and the lower half of a single smooth helical CRPC surface

Proof $X_0(s)$ and $X_1(s)$ are C^∞ in the domain $I_C = \left\{ s : s > 0, \frac{2Cs^{k+1}}{s^2+1} > 1 \right\}$ with respect to s. We now show that the complete contour curve is obtained by gluing curves $X_0(s)$ and $X_1(s)$ properly together (Fig. 4). To show this, we focus on the continuous function $h(s) = \frac{2Cs^{k+1}}{s^2+1}$, where $s \in [0, \infty)$. Since $h(0) = 0$ and $h(s) > 1$ for $s \in I_C$, by the Intermediate Value Theorem there exists a positive number $s_0 = \inf I_C$ such that $h(s_0) = 1$ or equivalently $2Cs_0^{k+1} = s_0^2 + 1$. No matter whether $k < 1$ or $k \geq 1$, it is easy to observe that the function $h(s)$ is strictly increasing at $s = s_0$ which gives $h'(s_0) > 0$ or equivalently $(k-1)s_0^2 + k + 1 > 0$. Since $g'(s)$ and $\sqrt{s^2+1}$ are

continuous near s_0, when $s \to s_0^+$ we have

$$\frac{g'(s)}{t(s)} = \frac{g'(s)\sqrt{s^2+1}}{\sqrt{2Cs^{1+k} - s^2 - 1}} = O\left(\frac{1}{\sqrt{2Cs^{1+k} - s^2 - 1}}\right) = O\left(\frac{1}{\sqrt{s - s_0}}\right).$$

The last equality holds because

$$\lim_{s \to s_0^+} \frac{2Cs^{k+1} - s^2 - 1}{s - s_0} = \lim_{s \to s_0^+} (2C(k+1)s^k - 2s) = \frac{(k-1)s_0^2 + k + 1}{s_0} > 0.$$

Again, the last equality holds because $2Cs_0^{k+1} = s_0^2 + 1$.

The above argument guarantees the existence of the integral $\int \frac{g'(s)}{t(s)} ds$ when $s \to s_0^+$. We may add a suitable constant to the $z-$coordinate of $X_1(s)$ s.t. $X_0(s_0) = X_1(s_0)$ and glue these two branches at this point. Intuitively, the entire curve should be smooth at the glued point since it satisfies the global CRPC property. The whole curve is derived from the solution of ODE (9) and $t(s_0) = 0$ is indeed a singularity of (9). However, by multiplying with t^2 on both sides one can easily find that the singularity is removable. Thus according to the theory of ODEs, the solution is smooth at $t = 0$ (i.e. $s = s_0$). $\square$

4 Shape analysis and classification

4.1 Top views of the profile curves

Helical CRPC surfaces are a generalization of helical minimal surfaces. For the latter, it is known that the profiles (contours for parallel projection orthogonal to the helical axis) appear as hyperbolas in the top view (Wunderlich 1952). Hence, it is natural to see how complicated the top views get for CRPC surfaces. We show the following result.

Proposition 5 *For any rational value of k, the top view of the profile curve $X_i(s)$ of a corresponding helical CRPC surface lies in an algebraic curve.*

Proof The top view of the profile is given by $(x, y) = (\pm t/2, g)$. Assume $k = \frac{n}{m}$ and notice that

$$t^2(s) + 1 = \frac{2Cs^{k+1}}{s^2 + 1}, \quad g^2(s) = \left(\frac{(k-1)s^2 - (k+1)}{4k}\right)^2 \frac{2Cs^{k-1}}{s^2 + 1}.$$

Thus both $(t^2(s) + 1)^m$ and $g^{2m}(s)$ are rational functions of s. In fact, there is a polynomial $P(t, g)$ such that $P(t(s), g(s)) = 0$, $\forall s$. More specifically, we have

$$\frac{g^2(s)}{t^2(s) + 1} = \frac{1}{16k^2}\left((k-1)^2 s^2 + \frac{(k+1)^2}{s^2} - 2(k^2 - 1)\right). \tag{11}$$

This quadratic equation in s^2 allows us to express s^2 in the form $s^2 = A + B$ where A, B^2 are rational functions of (t, g). Further, let

$$F := (t^2(s) + 1)^{2m} = \frac{(2C)^{2m}(s^2)^{n+m}}{(s^2 + 1)^{2m}} = \frac{P_1 + Q_1 B}{P_2 + Q_2 B}$$

where P_i, Q_i are rational functions of (t, g). This step can be simplified when m, n have the same parity, in which case

$$F := (t^2(s) + 1)^m = \frac{(2C)^m(s^2)^{\frac{n+m}{2}}}{(s^2 + 1)^m} = \frac{P_1 + Q_1 B}{P_2 + Q_2 B}.$$

Finally, since

$$B^2 = \left(\frac{P_1 - F P_2}{Q_1 - F Q_2} \right)^2$$

we get the desired polynomial by taking the numerator of

$$B^2(Q_1 - F Q_2)^2 - (P_1 - F P_2)^2 = 0.$$

$\square$

Remark 4 By Equ. (11) we can identify $t^2 + 1$ as common denominator of A and B, and thus all P_i, Q_i admit powers of $t^2 + 1$ as their denominators. By tracking the degree in each step of the proof, it is not hard to obtain $4(3m + n)$ *as an upper bound of the degree of the final algebraic curve.*

Example 1 We compute the top view of $X_0(s)$ for $k = 3$, based on the proof of Proposition 5. Omitting the details, we arrive at

$$\left(\frac{C}{3} - \frac{1}{16} - \frac{x^2}{4} - \frac{y^2}{4} \right) (4x^2 + 1)^2 - \frac{4C^2}{9} (4x^2 + 1) + 6Cy^2(4x^2 + 3y^2 + 1) = 0.$$

seeing that the curves are of algebraic order 6. They pass through the absolute points and possess contact of order 3 with the ideal line at the ideal point of the x-axis. Fig. 5 shows the resulting curves for different values of C.

4.2 Singularities

In a study of discrete CRPC surfaces, helical ones have been computed via numerical optimization (Wang and Pottmann 2022). There, it appeared that the positively curved ones among them should have singularities. However, the singularities could not be computed, since their formation has been prevented by fairness functionals which are required in that approach. Now, the presence of singularities is easy to see.
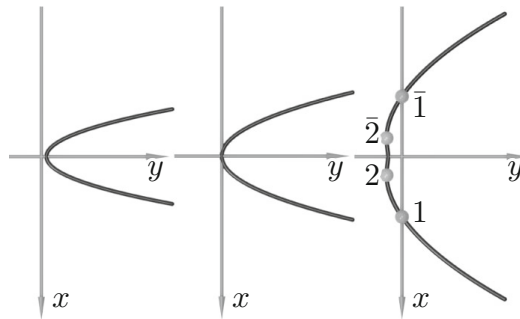
Fig. 5 Top views of the profile for $k = 3$ and different values of C. Left: $C = 1/8$; the contour lies on one side of the xz-plane. Middle: $C = 3/8$; the contour touches the xz-plane and the $z-$axis lies on the helical surface. Right: $C = 10$; the contour crosses the xz-plane. The path tangent T_p is in asymptotic direction at points 1, $\bar{1}$ and the contour tangent T_c is in asymptotic direction at points 2, $\bar{2}$

Proposition 6 *Positively curved helical CRCP surfaces possess singular curves.*

Proof $X_0'(s)$ has a common factor of each coordinate,

$$X_0'(s) = h'(s)\left(\frac{1}{4t(s)}, \frac{(k+1)s^2 - k + 1}{8ks\sqrt{h(s)}}, \frac{(k+1)s^2 - k + 1}{8kst(s)\sqrt{h(s)}}\right) \tag{12}$$

where

$$h'(s) = \frac{2Cs^k((k-1)s^2 + 1 + k)}{(s^2+1)^2}.$$

Thus a cusp occurs if $s = s_k = \sqrt{\frac{1+k}{1-k}}$, in which case we must have $k < 1$ (i.e. $a > 0$); see Fig. 6. In this case, $t(s)$ has a maximum at $s = s_k$ and then decreases until $t(s_0') = 0$ for some $s_0' > s_k > s_0$. With the same argument as in Proposition 4, we know that $X_0(s)$ and $X_1(s)$ can be glued smoothly at $s = s_0'$ (Fig. 4). If we keep the gluing procedure with a sequence of profiles, we obtain a periodic curve. This is illustrated in Fig. 7 for different values of k via the intersections of helical CRPC surfaces with the $(x, z)-$plane. $\qquad\square$

Under the helical motion, $X_0(s_k)$ generates a singular curve. In the next subsection, we will show that it is natural to consider the curvature ratio a switching to $1/a$ when moving across a singular helix. So, for convenience we split $X_0(s)$ into two curves $X_0^+(s)$, $s \geq s_k$ and $X_0^-(s)$, $s \leq s_k$.

One question arises: Do these two curves actually stop at $s = s_k$ or do they just share the same tangent here? In other words, can any of them, say $X_0^-(s)$, be continued a little bit to $s = s_k + \epsilon$ for some $\epsilon > 0$? The answer is no! Before a rigorous proof we would like to illustrate such a situation with a simple example.

Example 2 Consider the initial value problem

$$y'(x) = 1 + \sqrt{y(x)}, \quad y(0) = 0.$$

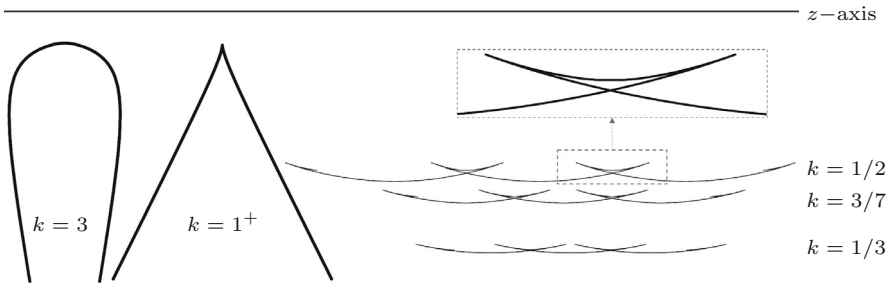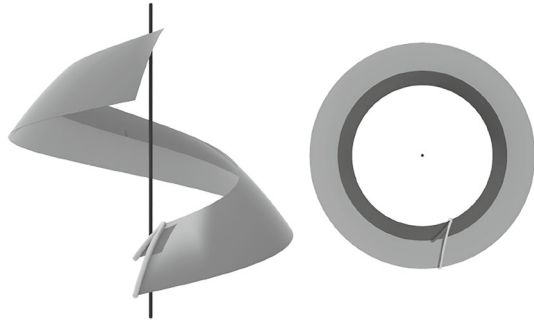**Fig. 6** Surface generated by X_0 near the cusp. Right: Top view

Fig. 7 Typical intersections of helical CRPC surfaces with planes through the helical axis. As $k \to 1^+$, the surface tends to a developable surface which is generated by the tangents of a helical path. As $k \to 1^-$, which is not shown in this graph, the surface tends to a cylinder, so the intersection is just a straight line parallel to the $z-$axis

By separation of variables, we obtain the implicit solution

$$2\sqrt{y(x)} - 2\ln\left(1 + \sqrt{y(x)}\right) = x .$$

This function is well defined in the first quadrant because it is monotone. But it is impossible to continue this solution at the origin since $y'(0) = 1$ and any continuation will cause a negative value for $y(x)$.

The above example can be generalized to our case, i.e. ODE (5):

Proposition 7 *A profile curve* $X_0(s)$*, as a solution of equation* (5)*, cannot be continued beyond a singularity* $X_0(s_k)$*.*

Proof If we set $w(t) = (t + \frac{1}{t})g'(t)$, (5) is a quadratic equation $1 + t^2 + (w + g)^2 = k^2(w - g)^2$ of w, which essentially consists of two equations. The two solutions meet each other when the discriminant $D(t, g) = 16k^2g^2 + 4(k^2 - 1)(1 + t^2) = 0$. We can show that $D(t(s_k), g(s_k)) = 0$.

On the other hand, although $X_0'(s_k) = 0$, the limit tangent at $s = s_k$ does exist. According to Equ. (12), the $x, y-$coordinates of a tangent vector are

$$T(s) = \left(\frac{1}{4t(s)}, \frac{(k+1)s^2 - k + 1}{8ks\sqrt{h(s)}}\right).$$

Noting $\nabla D = (8(k^2 - 1)t, 32k^2 g)$, we have

$$\left.\frac{\partial D}{\partial T}\right|_{s=s_k} = \nabla D(t(s_k), g(s_k)) \cdot T(s_k) = -6 - 2k^2 < 0.$$

This means that any continuation at $s = s_k$ will cause a negative value for $D(t, g)$. Thus, $X_0^-(s)$ cannot be continued at $s = s_k$. A similar argument applies to $X_0^+(s)$. $\square$

4.3 Shape classification

Finally, we aim at a classification of all helical CRPC surfaces with a given constant k. There is an important difference to the well-known case of rotational CRPC surfaces. There, the only parameter which influences the shape, is the constant curvature ratio a. In contrast, the shape of a helical CRPC surface does not only depend on k (recall $k = |1 - a|/|1 + a|$), but also on the constant C.

For convenience, we adopt the following basic setup.

(1) We focus on those points of the surface where individual solutions have been glued together. Their tangent planes are parallel to the helical axis. For positive curvature ($k < 1$), we have two such positions, associated with $s = s_0, s = s_0'$ respectively and we will use X^-, X^+ to clarify.

(2) We use $X(v, s)$ from Theorem 3 to represent the surface and when constant C is involved in the discussion, we write $X(v, s; C)$.

(3) Notice that near the glued point, t is a monotone function of s. This allows us to locally take t as the parameter. Thus the surface and the glued point are $X(v, t)$, $X(0, 0)$ respectively.[2]

(4) Any shift along the $z-$ axis will not change the shape of the surface. Hence we can assume that $X(0, 0)$ (or $X^-(0, 0)$ etc.) lies on the $y-$ axis.

The case of positive curvature. For $k < 1$, the helical path of the cusp splits the surface into two parts (see Fig. 7). It is easy to see that, when C varies, the outer part (denoted by $X^-(v, t)$, corresponding to the longer segments between two cusps in Fig. 7) stays outer and the inner part (denoted by $X^+(v, t)$, belonging to the shorter segments between two cusps in Fig. 7) stays inner. The classification is based on that, answering the question whether a part should be associated with curvature ratio a or $1/a$.

Distinguishing principal directions. The principal directions of a rotational surface are the tangents of its parallel circles and meridians. Thus, the associated principal curvatures can be labeled as κ_1 and κ_2 respectively. If we set $\kappa_1/\kappa_2 = a$ or $\kappa_1/\kappa_2 = 1/a$ for some constant $a \neq 0, \pm 1$, there will be two essentially different (i.e. non-similar) surfaces corresponding to each case (see e.g. Kühnel 2013; Wang and Pottmann 2022). However, up to now everything we discussed about helical CRPC surfaces is determined by the constant $k = |1 - a|/|1 + a| = |1 - \frac{1}{a}|/|1 + \frac{1}{a}|$, where the cases $\kappa_1/\kappa_2 = a$ and $\kappa_1/\kappa_2 = 1/a$ are not distinguished at all. We will now provide a way to label the principal curvatures.

---

[2] This new parameterization considerably reduces the calculation for derivatives in the light of ODE (9) when $t = 0$.

Proposition 8 *For a positively curved helical CRPC surface ($k < 1$), the ratio of normal curvatures κ_v/κ_t of the helical path and profile (contour) at the points with a tangent plane parallel to the helical axis tends to different values for the outer part X^- and the inner part X^+, when $C \to \infty$, namely*

$$\lim_{C \to \infty} \frac{\kappa_v^-}{\kappa_t^-} = \frac{1-k}{1+k}, \quad \lim_{C \to \infty} \frac{\kappa_v^+}{\kappa_t^+} = \frac{1+k}{1-k}. \tag{13}$$

This allows for a consistent labeling of principal curvatures as κ_1 and κ_2, leading to different curvature ratios a and $1/a$ for the outer and inner parts of the surface, which are separated by the singular helices.

Proof We have to compute the normal curvatures of $X(v, t)$ for the parameter lines at the point $X(0, 0)$. Recall that this point generates a helical path along which the CRPC surface is tangent to a co-axial rotational cylinder (see Fig. 4). The profile curve $X(0, t)$ and the helical path $X(v, 0)$ are symmetric with respect to the y-axis, on which $X(0, 0)$ lies. The helical tangent is $X_v(0, 0)$ and profile tangent is $X_t(0, 0)$.

Let κ_v^-, κ_t^- be the normal curvatures of $X^-(v, 0)$, $X^-(0, t)$ respectively, for which we find at $X^-(0, 0)$,

$$\frac{\kappa_v^-}{\kappa_t^-} = \frac{(1+k)s_0^4 + O(s_0^2) + 1 - k}{(1-k)s_0^4 + O(s_0^2) + 1 + k}.$$

If we let $C \to +\infty$, $X^-(0, 0)$ will tend to $-\infty$ along the y-axis. Since we have fixed the pitch at $1/2$, moving with $X^-(0, 0)$ to infinity, the surface becomes locally like a rotational one. The parameter curves $X^-(v, 0)$, $X^-(0, t)$ are locally like parallel circle and meridian. So the ratio of principal curvatures can be approximated by κ_v^-/κ_t^-. Similarly, the ratio for $X^+(v, t)$ can be approximated by

$$\frac{\kappa_v^+}{\kappa_t^+} = \frac{(1+k)s_0'^4 + O(s_0'^2) + 1 - k}{(1-k)s_0'^4 + O(s_0'^2) + 1 + k}.$$

Consider the way how we choose s_0 and s_0': The function $h(s) = \frac{2Cs_0^{1+k}}{s_0^2+1}$, $k < 1$ is firstly increasing and then decreasing on $[s_0, s_0']$ where $h(s_0) = h(s_0') = 1$. It is not hard to see that $C \to +\infty$ implies $s_0 \to 0$ and $s_0' \to +\infty$. Thus

$$\frac{\kappa_v^-}{\kappa_t^-} \to \frac{1-k}{1+k}, \quad \frac{\kappa_v^+}{\kappa_t^+} \to \frac{1+k}{1-k},$$

showing that we can treat $X^-(v, t)$, $X^+(v, t)$ as two different types of surfaces and assign curvature ratios $\frac{1-k}{1+k}$ and $\frac{1+k}{1-k}$, respectively, to them.

The above discussion provides a natural way to label the principal curvatures (including the case $a < 0$): For any surface $X(v, t; C)$, suppose we have an unlabeled principal frame at $X(0, 0; C)$. By increasing the value of C, this point is pushed to infinity and one of its principal directions continuously drives to the direction of

$X_v(0, 0; C)$. We label the principal curvature in this direction by κ_1 and the other by κ_2. □

Remark 5 In the case $a < 0$, we can copy all calculations from $X^-(v, t)$ and obtain

$$\frac{\kappa_v}{\kappa_t} = \frac{(1 + k)s_0^4 + O(s_0^2) + 1 - k}{(1 - k)s_0^4 + O(s_0^2) + 1 + k}.$$

However, it immediately follows that $\lim_{C \to +\infty} \frac{\kappa_v}{\kappa_t} = \frac{1-k}{1+k}$. Hence, all surfaces share one common ratio, on which we cannot base a classification.

Shapes for negative curvature. In order to classify the case $a < 0$, we consider the intersection of the surface and the yz-plane, which we call yz-profile. These profiles also show the essential distinction in the positively curved case, namely the shorter (inner) and longer (outer) segments between cusps (Fig. 7). For $a < 0$, we get essentially three types of shapes, seen in Fig. 8. The figure only shows the essential part of the profile, which we call the *generating profile*. The complete yz-profile is obtained from the generating profile by application of those reflections at the helical axis and translations parallel to it which correspond to rotation angles $v = n\pi, n \in \mathbb{Z}$, in the helical motion. This entire pattern shows a nice transition between the three cases, supporting the completeness of the classification.

The yz-profile generates the same surface as $X(0, t)$ does. But for different values of C, the yz-profiles can be classified into three major cases (see Figs. 5 and 8). The separating case corresponds to the middle image of Fig. 5. It belongs to $s_0 = \sqrt{(k + 1)/(k - 1)}$, or equivalently, since $h(s_0) = 1$,

$$C = C_k := \frac{k(k - 1)^{\frac{k-1}{2}}}{(k + 1)^{\frac{k+1}{2}}}. \tag{14}$$

Proposition 9 *The elementary yz-profile of a negatively curved helical CRPC surface can have the following shapes, depending on the value of the constant C. (a) For $C \in (0, C_k)$, the profile can be written as graph $y = F(z)$ of a positive even function F. (b) For $C = C_k$, the profile is the graph $z = G(y)$ of an odd function G. (c) For $C > C_k$, the profile lies on one side of the z-axis and is symmetric with respect to the y-axis, on which it has a self-intersection.*

Proof For $C \in (0, C_k)$, i.e. $s_0 > \sqrt{\frac{k+1}{k-1}}$, $g(s)$ is always positive. As we can see from Fig. 5 left, the top view of $X_0(s)$ lies in the first quadrant. To get the upper half of the yz-profile, we need to move each point $X_0(s) = \left(\frac{t(s)}{2}, g(s), \int \frac{g'(s)}{t(s)} ds \right)$ along its helical path until it reaches the yz-plane. The corresponding coordinate on the yz-profile is

$$\left(0, \sqrt{\frac{t(s)^2}{4} + g(s)^2}, \int \frac{g'(s)}{t(s)} ds + \frac{1}{2} \tan^{-1} \frac{t(s)}{2g(s)} \right).$$

Similarly, the point $\left(-\frac{t(s)}{2}, g(s), -\int \frac{g'(s)}{t(s)} ds\right)$ on $X_1(s)$ must be moved backwards to the yz-plane, and the corresponding coordinate on the lower half of the yz-profile is

$$\left(0, \sqrt{\frac{t(s)^2}{4} + g(s)^2}, -\int \frac{g'(s)}{t(s)} ds - \frac{1}{2} \tan^{-1} \frac{t(s)}{2g(s)}\right).$$

If we fix $X(0, 0)$ on the $y-$axis, then this yz-profile is smooth and symmetrical with respect to the $y-$axis (Fig. 8 left). Finally, by computing the derivative of the third coordinate from the upper half, its numerator admits the factorization

$$C(k^2 - 1)s^{2k-1}(s^2 + 1)((k - 1)x^2 + k + 1)((k - 1)s^2 - k - 1),$$

which is always positive given that $s \geq s_0 > \sqrt{\frac{k+1}{k-1}}$. Having no tangent orthogonal to the z-axis, the curve is the graph of a function $y = F(z)$.

For $C > C_k$ i.e. $s_0 < \sqrt{\frac{k+1}{k-1}}$ (Fig. 5 right), $X(0, 0)$ lies on the negative part of the $y-$axis. Now the points on $X_0(s)$ should be moved backwards and the points on $X_1(s)$ should be moved forward. $X_0(s)$ contributes half of the yz-profile. If we choose the branch of $\cot^{-1}(x)$ whose range lies in $(-\pi, 0)$, the expression can be given by

$$\left(0, -\sqrt{\frac{t(s)^2}{4} + g(s)^2}, \int \frac{g'(s)}{t(s)} ds + \frac{1}{2} \cot^{-1} \frac{2g(s)}{t(s)}\right).$$

The complete yz-profile is obtained by reflecting the above curve at the y-axis. In this case, the yz-profile possesses a self-intersection at the y-axis (Fig. 8 right). This is shown as follows. The highest degree of s in $g'(s)$ and $t(s)$ is the same. This means $\frac{g'(s)}{t(s)}$ tends to a (positive) constant when $s \to +\infty$. Since $\tan^{-1} \frac{t(s)}{2g(s)}$ is bounded, $\left(\int \frac{g'(s)}{t(s)} ds - \frac{1}{2} \tan^{-1} \frac{t(s)}{2g(s)}\right) \to +\infty$ when $s \to +\infty$. On the other hand, one can show that the derivative $\left(\int \frac{g'(s)}{t(s)} ds - \frac{1}{2} \tan^{-1} \frac{t(s)}{2g(s)}\right)'_s \to -\infty$ when $s \to s_0^+$. These calculations guarantee that the curve will cross the $y-$axis, i.e. possess a self-intersection.

For $C = C_k$, i.e. $s_0 = \sqrt{\frac{k+1}{k-1}}$ (Fig. 5 middle), $X(0, 0)$ coincides with the origin and the tangent at this point lies on the xz-plane. This implies $\lim_{s \to s_0^+} \tan^{-1} \frac{t(s)}{2g(s)} = \frac{\pi}{2}$. So for convenience, we consider the xz-profile instead, which is tangent to $X(0, t)$ at the origin. Again, $X_0(s)$ contributes half part of it, which is

$$\left(\sqrt{\frac{t(s)^2}{4} + g(s)^2}, 0, \int \frac{g'(s)}{t(s)} ds - \frac{1}{2} \tan^{-1} \frac{2g(s)}{t(s)}\right).$$
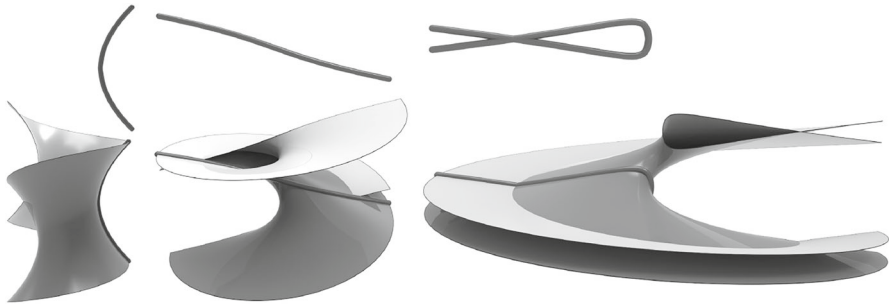
Fig. 8 The shapes of CRPC surfaces to a curvature ratio $a < 0$ (here $k = 3$) depend on the value of C. Left: $C = 0.01$. Center: $C = C_k = 3/8$. Right: $C = 1$

The other half from $X_1(s)$ is

$$\left(-\sqrt{\frac{t(s)^2}{4} + g(s)^2}, 0, -\int \frac{g'(s)}{t(s)}\,ds + \frac{1}{2}\tan^{-1}\frac{2g(s)}{t(s)} \right).$$

Together they form an odd (smooth) function in the xz-plane (Fig. 8 middle). Clearly, the yz-profile is congruent to it and obtained by applying the helical motion with an angle of 90 degrees. □

Future work

One direction for future research is the determination of all spiral CRPC surfaces, as extensions of the known spiral minimal surfaces (Wunderlich 1954). This is a natural question, since CRPC surfaces are invariant under Euclidean similarities and spiral surfaces are generated by one parameter subgroups of the Euclidean similarity group. The present approach based on profiles for projection orthogonal to the spiral axis should be promising, since these profiles also appear in Wunderlich's spiral minimal surfaces (Wunderlich 1954). However, the characterizing ODE is much more complicated and thus we leave its solution for future work.

The determination of explicit representations for CRPC surfaces apart from the so far mentioned ones is a bigger challenge, as it amounts to the solution of a rather complicated nonlinear partial differential equation. A geometric construction of general CRPC surfaces can be based on a Christoffel-type transformation of the Gaussian spherical image (Jimenez et al. 2020), but it remains open whether this is a path towards explicit parameterizations of CRPC surfaces.

References

Hopf, H.: Über Flächen mit einer Relation zwischen den Hauptkrümmungen. Math. Nachr. **4**, 232–249 (1951)

Jimenez, M.R., Müller, C., Pottmann, H.: Discretizations of surfaces with constant ratio of principal curvatures. Discrete Comput. Geom. **63**(3), 670–704 (2020)

Kühnel, W.: Differentialgeometrie, updated edn. Aufbaukurs Mathematik, p. 284. Springer, Wiesbaden . Kurven—Flächen—Mannigfaltigkeiten (2013)

López, R.: Linear Weingarten surfaces in Euclidean and hyperbolic space. Mat. Contemp. **35**, 95–113 (2008)

Lopez, R., Pampano, A.: Classification of rotational surfaces in euclidean space satisfying a linear relation between their principal curvatures. Math. Nachr. **293**, 735–753 (2020)

Mladenov, I.M., Oprea, J.: The Mylar balloon revisited. Amer. Math. Monthly **110**(9), 761–784 (2003)

Mladenov, I.M., Oprea, J.: The mylar ballon: new viewpoints and generalizations. In: Proceedings of the Eighth International Conference on Geometry, Integrability and Quantization, pp. 246–263 (2007)

Pellis, D., Kilian, M., Wang, H., Jiang, C., Müller, C., Pottmann, H.: Architectural freeform surfaces designed for cost-effective paneling through mold re-use. In: Advances in Architectural Geometry 2020, pp. 2–16. Presses des Ponts (2021a)

Pellis, D., Kilian, M., Pottmann, H., Pauly, M.: Computational design of Weingarten surfaces. ACM Trans. Graphics **40**(4), 111–114 (2021b)

Riveros, C.M.C., Corro, A.M.V.: Surfaces with constant Chebyshev angle. Tokyo J. Math. **35**(2), 359–366 (2012)

Riveros, C.M.C., Corro, A.M.V.: Surfaces with constant Chebyshev angle II. Tokyo J. Math. **36**(2), 379–386 (2013)

Schling, E., Kilian, M., Wang, H., Schikore, D., Pottmann, H.: Design and construction of curved support structures with repetitive parameters. In: Hesselgren, L., Kilian, A., Malek, S., Olsson, K.-G., Sorkine-Hornung, O., Williams C. (eds.) Advances in Architectural Geometry, pp. 140–165. Klein Publishing Ltd (2018)

Stäckel, P.: Beiträge zur Flächentheorie. III. Zur Theorie der Minimalflächen. Leipziger Berichte, 491–497 (1896)

Tellier, X., Douthe, C., Hauswirth, L., Baravel, O.: Caravel meshes: a new geometrical strategy to rationalize curved envelopes. Structures **28**, 1210–1228 (2020)

Wang, H., Pottmann, H.: Characteristic parameterizations of surfaces with a constant ratio of principal curvatures. Comp. Aided Geom. Design **93**, 102074 (2022)

Weingarten, J.: Über eine Klasse aufeinander abwickelbarer Flächen. J. reine u. angewandte Mathematik **59**, 382–393 (1861)

Wunderlich, W.: Beitrag zur Kenntnis der Minimalschraubflächen. Compos. Math. **10**, 297–311 (1952)

Wunderlich, W.: Beitrag zur Kenntnis der Minimalspiralflächen. Rend. Math. **13**, 1–15 (1954)